ELSEVIER

Mechanics of Materials 30 (1998) 217–227

MECHANICS OF MATERIALS

The influence of temperature on dynamic failure mode transitions

D. Rittel [1]

Faculty of Mechanical Engineering, Technion Israel Institute of Technology, 32000 Haifa, Israel

Received 31 March 1997; received in revised form 9 April 1998

Abstract

A failure mode transition from opening to shear has been reported in shear impact experiments of commercial polycarbonate with increasing impact velocity (Ravi-Chandar, K., 1995. On the failure mode transitions in polycarbonate under dynamic mixed mode loading. Int. J. Solids and Structures 32 (6/7), 925–938; Rittel, D., Levin, R., Maigre, H., 1997. On dynamic crack initiation in polycarbonate under mixed-mode loading. Mech. Res. Comm. 24 (1), 57–64). Impact velocities ranged typically from 20 to 60 m/s and the experiments were carried out at room temperature. Similar transitions have been reported for metallic materials and shear band formation at high velocities has been related to crack-tip adiabatic heating and material softening. This paper investigates the role of crack-tip heating in the observed trans ition. Results are reported and discussed for *high velocity* (50–60 m/s) shear impact experiments of commercial polycarbonate whose *temperature* is varied in the range of −120°C to +70°C. Up to −40°C, fracture proceeds along an initial kink angle of typically 60°. At −25°C the kink angle is reduced to 40° and less. At room temperature and above, the specimens no longer fracture by separation. A 2–3 mm shear band is then clearly noticeable at the crack-tip. Scanning electron and optical fractographic examination of the specimens confirm the initial operation of a shear fracture mechanism at −25°C ($T_{eq} = 0.59\ T_g$ in [K]), in contrast with an opening fracture mechanism at lower temperatures (crazing). Assuming that shear failure results from local heating above the glass transition temperature (150°C), the crack-tip temperature elevation is estimated to be at least 175°C. Significant crack-tip temperature changes put limitations on the usual assumptions of isothermal dynamic crack initiation. © 1998 Elsevier Science Ltd. All rights reserved.

Keywords: Dynamic fracture; Failure mode transitions; Polymeric materials; Glassy transition; Fractography

1. Introduction

A series of recent studies has disclosed a failure mode transition for notched (cracked) plates subjected to transient dynamic loading parallel to the notch line. Specifically, two ranges of impact velocities (“lower” and “higher”) have been investigated. The experiments show the operation of an opening type of failure at the lower impact velocities whereas at the higher impact velocities an adiabatic shear band forms at the crack-tip and fracture proceeds along the initial crack-line (sometimes it may not progress at all). The transition has been reported in maraging steel (Kalthoff, 1988; Mason et al., 1994; Zhou et al., 1996a, b) and also in commercial polycarbonate (Ravi-Chandar, 1995). Consequently, the dynamic failure mode transition is not limited to one kind

[1] E-mail: rittel@dany.technion.ac.il

0167-6636/98/$ – see front matter © 1998 Elsevier Science Ltd. All rights reserved.
PII: S0167-6636(98)00043-X

of (crystalline) material as it appears in an amorphous thermoplastic polymer as well.

Furthermore, the development of adiabatic shear bands at the crack-tip is not restricted to the above mentioned kind of experiments which were analyzed in detail by Lee and Freund (1990). The general phenomenon can be related to mixed-mode loading conditions which prevail at the crack-tip. In this context, Rittel et al., 1997; Rittel and Levin (1998) investigated the dynamic fracture of commercial polycarbonate subjected either to dominant mode I (compact compression specimens) loading or to dominant mode II (shear impact) loading. Their analysis relied on small scale yielding linear elastic fracture mechanics. The experimental results were processed using numerical simulations of the experiments in which contact between the fatigue crack faces was taken into account.

For (mixed-mode) dominant mode II experiments it was found that the main role of the contact between the crack faces is to cancel the negative mode I component which characterizes this kind of experiments (Lee and Freund, 1990). The crack-tip experiences almost pure mode II loading initially, followed by mixed-mode loading at later times upon arrival of reflected waves. An opening to shear transition similar to that previously reported was observed when the impact velocity was raised from less than 30 m/s to more than 50 m/s. In the first case, the specimens fractured by separation a typical kink angle of about 40° with respect to the crack-line. At the high impact velocities, the specimens did not fracture. Rather, they exhibited a clearly visible shear band at the crack-tip. Rittel et al., 1997; Rittel and Levin (1998) explained the transition by assuming a critical value of mode II stress intensity factor (K_{IISB}) at these high loading rates.

For their (mixed-mode) mode I experiments, all the specimens fractured but it was observed that despite the enforced dominant mode I, signs of shear banding were apparent in these cases where K_{IISB} was exceeded (high velocity impact). In such cases, the crack was observed to initially propagate by a shear mechanism over a few hundred microns. Then fracture proceeded by an opening type of failure identified as crazing.

It is therefore clear that *temperature variations are instrumental in the failure mode transition* and it is desirable to have an idea of the amplitude of the phenomenon. Zhou et al. (1996a, b) modeled the shear band formation using coupled thermomechanical calculations allowing for the softening of the material surrounding the crack-tip. These authors showed that a significant fraction of the melting temperature of the material can be reached in a thin layer ahead of the crack-tip. Measurements of transient crack-tip temperature fields are quite delicate to perform (see e.g. Zhender and Rosakis, 1991). However, useful estimates can be obtained, albeit in average form, by testing specimens at different global temperatures, as shown in this paper.

Motivated by our observations of shear band formation in high velocity/room temperature experiments, we now keep the *impact velocity relatively constant* in the "high velocity" regime while the specimens' *global temperature* is systematically varied. Consequently, this work investigates the failure mode transitions of side impacted specimens whose temperature lies in the −120°C to +70°C range. The chosen material is the previously investigated commercial polycarbonate for which the glass transition temperature is $T_{\mathrm{g}} = 150°\mathrm{C}$ (Ravi-Chandar, 1995). The extent to which the transition is observed provides additional experimental information on the local crack-tip temperatures involved in the failure mode transition.

The paper is organized as follows: first, we describe the experimental and numerical framework used in this work. Next, we report and discuss the experimental results on the failure mode transition and the characterization of the failure mechanisms. Conclusions are then drawn.

2. Experimental and Numerical

2.1. Experimental

2.1.1. Impact apparatus

The experimental setup is described in Fig. 1. A 12.7 mm diameter instrumented (PH 17-4) steel bar is brought in contact with the specimen (12.7 mm thick cracked plate) on one side. On its other side it

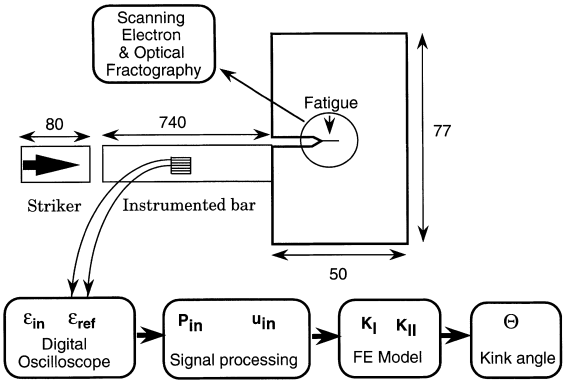

Fig. 1. Schematic representation of the shear impact experimental setup and data processing chain. All dimensions are in mm. The strain gage signals are collected on a high speed digital oscilloscope, processed into interfacial force and displacement signals. Next the force signal is fed into a numerical model to determine the evolution of the stress intensity factors. Finally, this evolution is used to determine the (kink) angle corresponding to the maximum hoop stress.

is impacted by a striker fired by a gas gun. Typical impact velocities can be adjusted in the 8–60 m/s range. The striker length is 8 cm which causes an impact duration of 30 μs. The striker induces a compressive pulse (ε_{in}) in the bar which is partly transmitted to the specimen and partly reflected as a tensile pulse (ε_{ref}). The pulses were collected by means of a digital oscilloscope (Nicollet 490 model) at a sampling rate of 5 MHz. The experimental pulses were corrected for geometrical dispersion (Kolsky, 1963; Lifshitz and Leber, 1994) using home made programs. Following determination of the incident and reflected pulses, the interfacial force P_i and velocity V_i pulses were determined using standard relations (Kolsky, 1963). In all the experiments the specimen lay unsupported so that fracture was purely inertial.

The experimental material was polycarbonate, supplied as 12.7 mm thick sheets. In each specimen, a fatigue crack was grown carefully such as to minimize the damage which accumulates at the crack-tip. The typical fatigue extension was about 2–3 mm long.

2.1.2. Assessment of the specimen's temperature

A cracked specimen was instrumented with a pair of thermocouples (J iron-constantan type). One thermocouple was cemented using a thin epoxy layer to the surface of the specimen in the vicinity of the crack-tip. The other thermocouple was cemented at specimen's mid-thickness in a small hole which was subsequently filled with epoxy based cement too. These two thermocouples were used to characterize the evolution of the surface and core temperatures of our polycarbonate specimens upon cooling or heating from a given temperature.

2.2. The numerical model

The experimental results are analyzed in the framework of two-dimensional small scale yielding linear elastic fracture mechanics. The crack-tip fields are characterized by the stress intensity factors (SIF) K_I and K_{II}. In our experiments, we do not monitor the crack-tip directly. Rather, we use a hybrid experimental–numerical approach (Kobayashi, 1987) in which the boundary conditions (experimental forces in this case) are prescribed to a finite element model of the specimen. The evolution of the SIF is determined from the motion of keypoints in the vicinity of the crack-tip (Bui et al., 1992).

The experiments were analyzed using a commercial finite element code (ANSYS, 1994). We assumed two-dimensional plane strain deformations and linear elastic material behavior. The crack-tip is modeled using singular quarter point elements (Barsoum, 1978) and the crack in all the analyses is kept *stationary* so that the SIF are a function of time only (Freund, 1990). Traction free conditions are assumed over all the specimen except at the specimen-bar interface. To simulate the experiment, the recorded force pulse (P_i) is applied to this interface as boundary condition. The specimen can separate from the bar in an actual experiment and separation is modeled as traction-free conditions. Consequently, the calculation can be extended beyond contact time for any duration wanted. An example of such recorded force pulse is shown in Fig. 2. The equations of motion were solved using Newmark's implicit scheme (Bathe, 1982).

As in our previous work, contact was modeled using special contact elements which apply a

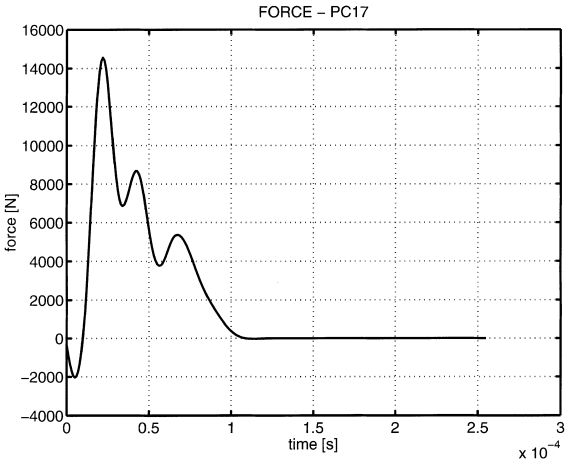

Fig. 2. Typical experimental (filtered) force pulse.

normal reaction when the gap between the two surfaces is closed. Friction was modeled as Coulomb friction and the coefficient of friction in all the analyses was chosen as $\mu s = 0.4$. This value is arbitrary as we do not know the actual coefficient of friction between the crack-faces. Yet the exact value is not critical for *stationary cracks* since our previous results showed that the dominant role is played by contact rather than by friction. Indeed, contact avoids interpenetration of the crack-flanks thus creating a loading configuration of almost "pure mode II" for a large part of the experiment while friction does not significantly affect the evolution of the SIF's.

A limited assessment of the temperature dependence of the mechanical properties of our polycarbonate is described next.

3. Results

3.1. Mechanical properties of polycarbonate

The mechanical properties of this material were assessed using quasi-static tensile testing (Table 1). An equivalent "transfer modulus" (to account for dynamic effects – see Rittel and Maigre, 1996a) was determined from longitudinal wave velocity measurements using ultrasonic technique. The measurements were carried out on a 5 mm thick disk to overcome attenuation problems characteristic of this material. The same procedure was also used to measure the longitudinal wave velocity in a specimen which was previously cooled in liquid nitrogen. For this specimen, the accurate temperature was not precisely known but we observed that the wave velocity did not vary by more than 15% in the cold material. This shows qualitatively that the elastic properties of the material are not markedly affected by temperature in the glassy state up to room temperature. We did not investigate the elastic properties of polycarbonate in the range 20–70°C and assumed them to be constant, in accord with available data on the flexural modulus of this material (Elsevier Materials Selector, 1991).

Table 1
Measured room temperature mechanical properties of the investigated polycarbonate

	Young's modulus (GPa)	Poisson's ratio
Static	2.43	0.37
Dynamic	3.72	0.37

3.2. Thermal response of the specimens

The evolution of the core and surface temperature of the specimens is shown in Fig. 3 for two distinct cases: heating from liquid nitrogen temperature, and cooling after extraction from boiling water. From these figures, it can be noted that the surface of the specimen behaves differently from its core, as expected. Since polycarbonate is a poor thermal conductor, we assumed that the surface layer is of limited depth which can be neglected to a first approximation with respect to the specimen's thickness. Consequently, the quoted temperatures were determined from the core readings.

3.3. Dynamic fracture as a function of temperature

It must be recalled here that previous room temperature (typically 23°C) high velocity/side impact of identical specimens showed the development of an adiabatic shear band and fracture did not progress significantly (Ravi-Chandar, 1995; Rittel et al., 1997; Rittel and Levin, 1998). For the sake of brevity we will not repeat in

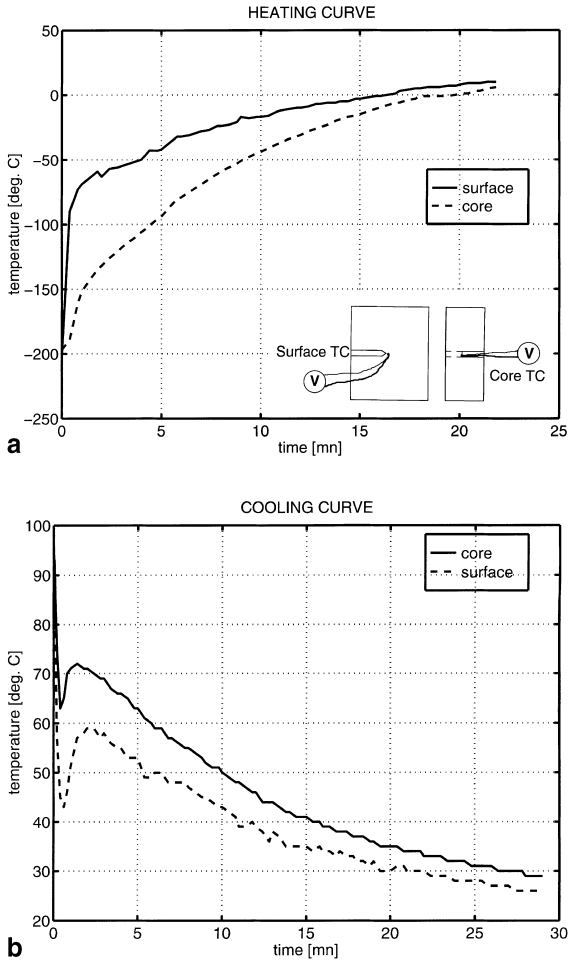

Fig. 3. Temperatures recorded by the core and surface thermocouples upon (a) heating, (b) cooling.

this paper the results obtained at room temperature.

The experimental results are listed in Table 2. A total of 9 specimens were fractured at a typical impact velocity ranging from 50 to 60 m/s. In the present experiments, the temperature of the specimens was varied between −120°C and +70°C. Therefore testing was carried below the glassy transition of this material. For all the specimens, the initial fracture (kink) angle was measured on both sides of the specimen. In some specimens it can be noted that the fatigue cracks did not grow symmetrically. In such cases, the crack length for calculation purposes was taken as the average value of the measurements. This lack of symmetry did not affect the experimental results reported here.

The results show that for *almost identical impact velocities the specimens react quite differently according to the global temperature of the material*:

- All the specimens tested in the range −120°C to −25°C fractured by separation.
- In contrast, the specimens tested at (RT) – 70°C did not fracture and developed noticeable shear bands (Figs. 4 and 5).
- Another interesting point is that in the fractured group, the initial kink angle remains remarkably constant in the temperature range of −120°C to −40°C and its typical value is 60° and above. At −25°C this angle becomes much smaller, inferior to 40° (Fig. 4). Ultimately, the kink angle vanishes and fracture no longer happens as the temperature is increased. The 70°C specimen exhibits a 2–3 mm long noticeable shear band in the extension of the crack-tip (Fig. 5).

Table 2
Experimental results. Note the kink angle transition at −25°C. Crack length and kink angle are measured on both sides of the specimen

Specimen	Temperature (°C)	V impact (m/s)	Crack-length (mm)	Kink angle (°)
PC16	−120	58	16.2–14.3	60–68
PC17	−90	55	14.4–15.7	56–51
PC20	−60	60	15.4–17.2	54–58
PC21	−40	60	16.4–15.7	55–58
PC22	−25	53	14.3–17.6	40–38
PC24	−25	53	16.3–17.5	33–30
PC28	−5	50	16.8–15.6	29–30
PC25	70	60	16.5–16.2	No fracture
PC27	70	60	17.5–15.7	No fracture

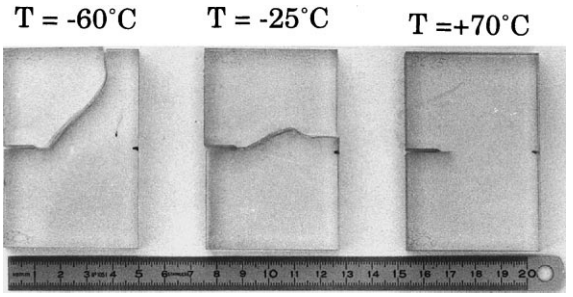

Fig. 4. Impacted specimens. (a) $T = -60°C$, (b) $T = -25°C$ and (c) $T = +70°C$. Note that the kink angle decreases with increasing specimen's temperature. Specimen (c) did not fracture. Impact velocities in the range of 50–60 m/s.

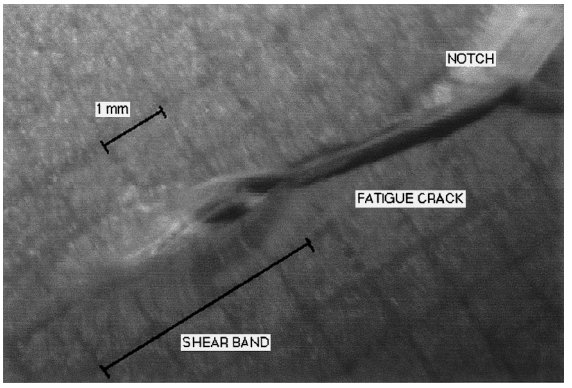

Fig. 5. Close-up view on the shear band generated at the crack-tip of a specimen at $T = +70°C$. Note the "flame-like" aspect of the shear band. The picture is taken perpendicular to the specimen laying on millimetric paper.

In Fig. 6, we show the results of the numerical simulation of three characteristic experiments, at extreme temperatures and in the mid-temperature range. Each experiment differs from the other in its exact experimental conditions of impact velocity, contact conditions and (temperature related) mechanical impedance which affect the transfer of energy to the specimen. Consequently, a straightforward comparison of the absolute values of the reported SIF should not be attempted. However, it must be noted that the overall *evolution* of the SIF's is rather similar in all cases. For such typical evolution, the loading starts mostly under pure mode II conditions during about the first 130 μs. Past this time, a marked mode I contribution appears, thus causing mixed-mode crack-tip loading.

The fracture surfaces of the specimens were investigated using scanning electron microscopy and characteristic fractographs are shown in Figs. 7 and 8 for a specimen fractured at −90°C (PC17) and another at −25°C (PC22). For the first specimen, fracture proceeds by a series of mirror-like parabolas which emanate from the crack-tip. These parabolas extend over typically 500 μm. Beyond this area, fracture progresses by displaying the characteristic periodic pattern which has been associated with crazing fracture mechanism (Washabaugh and Knauss, 1993 (in PMMA); Ravi-Chandar, 1995 (in PC)). Similar patterns were also observed by Rittel and Levin (1998) in their experiments. This observation shows the operation of a tensile fracture mechanism to which crazing is related (Ward and Hadley, 1993). The parabolas which are quite visible at low magnification do not reveal much significant features at much higher magnifications, as shown in Fig. 7.

Considering now the next specimen, PC22, the same general features are observed, i.e. occurrence of parabolas followed by crazing markings. However *one major difference* between the two specimens is noticeable. A layered band, typically 200 μm wide, is clearly visible between crack-tip and the parabolas. Such a band has been identified previously by Rittel et al. (1997) as the manifestation of a fractured adiabatic shear band. Higher magnification of this specific area disclose elongated voids (dimples) such as those observed by Ravi-Chandar (1995) and by Rittel and Levin (1998). Consequently, the fractographic examination reveals the operation of a shear failure mechanism inside adiabatic shear bands at −25°C. This is the first operating fracture mechanism prior to crack opening as shown by the crazing markings further along the crack path. It must be emphasized that the observation of a shear band also coincides with a marked change in the fracture angle.

4. Discussion

The key point of this work is the investigation of local crack-tip temperature elevations as a result of transient loading conditions. In order to get a

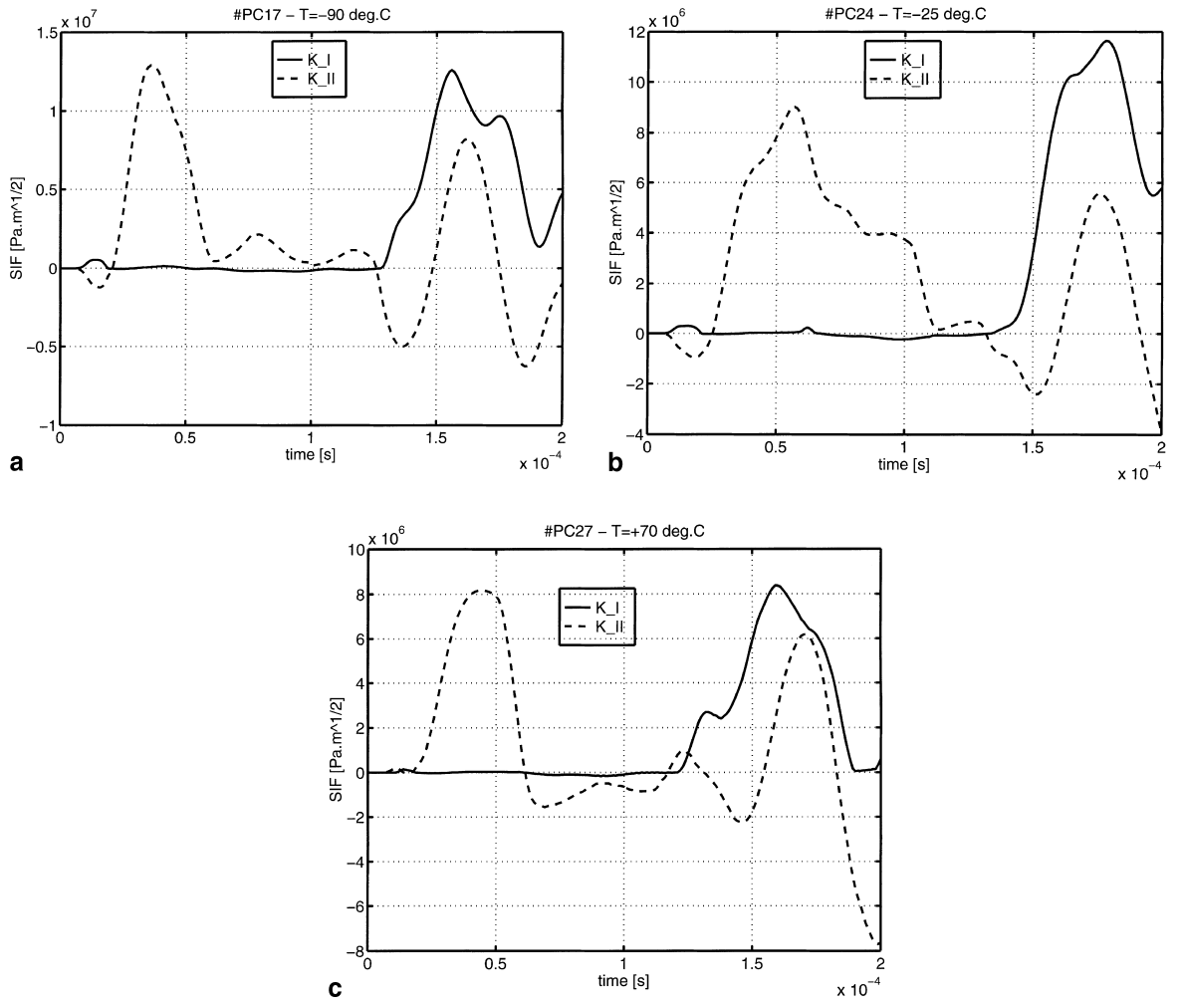

Fig. 6. Simulations of three experiments. (a) PC17 at −90°C, (b) PC24 at −25°C and (c) PC27 at 70°C. Note that the temporal evolutions of K_I and K_{II} are rather similar in all cases. Loading starts under almost pure mode II and mixed-mode is experienced after about 130 μs.

simple estimate of the phenomenon, the baseline (i.e. global) temperature of the specimen is controlled at the time of impact while the *local* crack-tip temperature is solely dictated by the thermomechanical response of the material. By reference to a "threshold temperature (T_g)", the local temperature elevation is thereby assessed in a very simple way.

The experiments reported in this paper shed additional light on the transition of failure modes. The specimens are loaded at "high" impact velocities yielding generally similar evolutions of K_I and K_{II}. Yet, radically different failure mechanisms are activated as a function of the global temperature of the material. Let us recall here that previous experimental measurements and numerical estimates of the temperature field in and around adiabatic shear bands have shown that a significant fraction of the melting temperature of the material can be reached (Zhou et al., 1996b).

Our experiments show in a simple and straightforward manner the role of thermally activated failure processes in this material. For a given T_g of 150°C, the observation of adiabatic

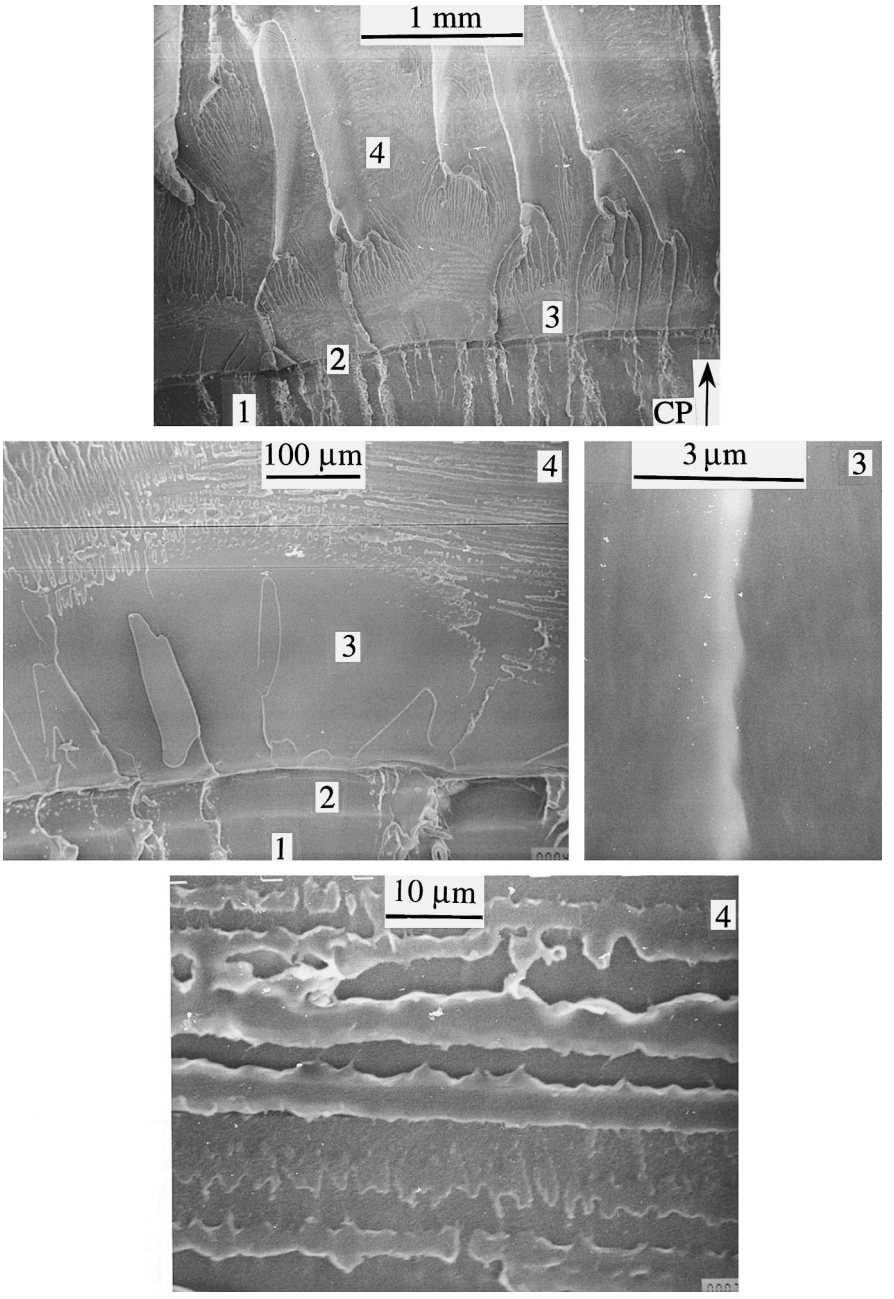

Fig. 7. Scanning electron fractograph of specimen PC17 ($T=-90$°C). Characteristic areas are indicated by numbers: 1 is the original fatigue crack. 2 is a featureless very narrow zone at which the crack starts to propagate by making a high kink angle with respect to 1. Area 3 corresponds to parabolic markings. Finally, area 4 contains crazing markings indicating fracture dominated by a normal stress. CP indicates crack propagation direction.

shear banding at −25°C ($T_{eq}=0.59\ T_g$ in [K]) provides a first estimate (lower bound) of the temperature elevation, i.e. 175°C. This is of course an averaged measurement as compared with local

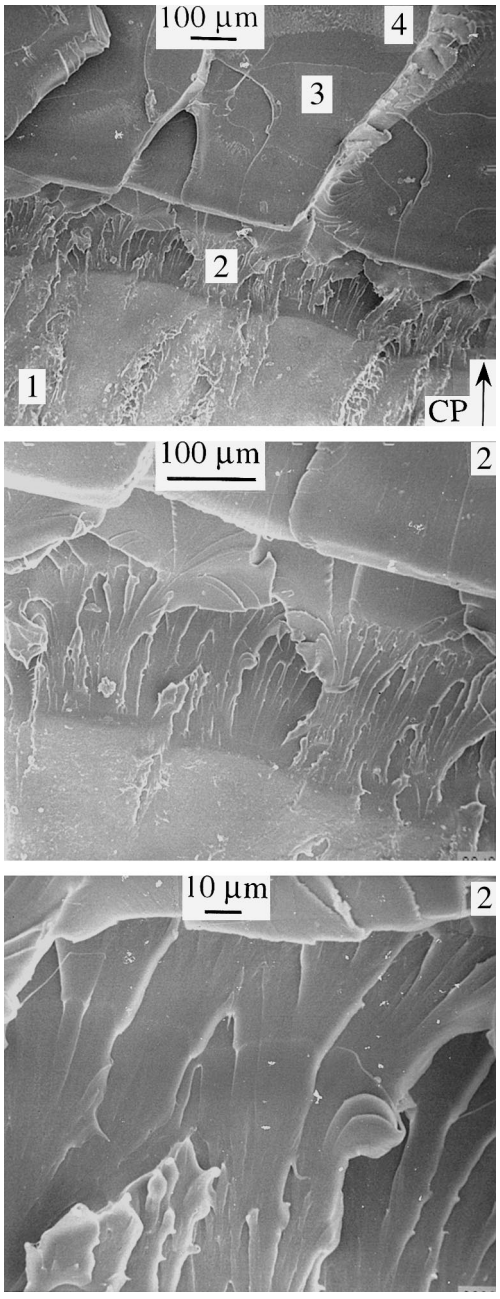

Fig. 8. Scanning electron fractograph of specimen PC22 ($T=-25$°C). Note the general resemblance to Fig. 7. As previously, 1 is the original fatigue crack, 3 and 4 indicate parabolic markings and crazing areas respectively. Note the new layer marked 2 which contains elongated markings indicative of a shear failure mechanism. Area 2 is the adiabatic shear band, about 200 μm wide.

recordings of the temperature field e.g. as in Zehnder and Rosakis (1991). Yet, the present experiments have the advantage of providing useful information in an independent and straightforward manner. The detection of the adiabatic shear band is supported by the fractographic analysis which clearly shows the operation of a shear failure mechanism.

The baseline temperature of −25°C is a turnpoint from which a noticeable change in the failure mechanism(s) is observed. This transition of failure modes is accompanied by a characteristic drop in the initial kink angle. Below the transition, the angle is of the order of 60°, then with increasing temperature the kink angle decreases and ultimately vanishes as a shear band is formed almost in the continuation of the original crack-line. In this respect, the experiments carried out a temperature exceeding RT do not yield much additional information as to the transition itself.

The kink angle values can be addressed within the framework of (small scale yielding) linear elastic fracture mechanics. The transition from opening to shear type of failure shows that the material surrounding the crack-tip has undergone some transformation (softening) which locally increases the fracture toughness of the material. As long as this transformation occurs on *a limited scale*, we assume that LEFM assumptions hold. We can thus use a macroscopic failure criterion, such as that of a maximum opening stress to identify the potential failure direction (kink angle). The angular values can be analyzed using a maximum (potential) energy release rate criterion. Such criterion was shown by Nuismer (1975) to be equivalent to a maximum hoop stress criterion $\max\{\sigma_{\Theta\Theta}\}$ (Lawn, 1995).

To illustrate this point, we have plotted in Fig. 9 the angle corresponding to the maximum hoop stress at each time step for a typical evolution of the SIF (such as shown in Fig. 6). During the initial pure mode II phase, the maximum hoop stress angle is of about 70° which is close to Lee and Freund's results (1990). No shear band was observed in this case.

Different angular values, in particular 40°, correspond to the later stages of the loading where mixed-mode is fully developed. In these cases a

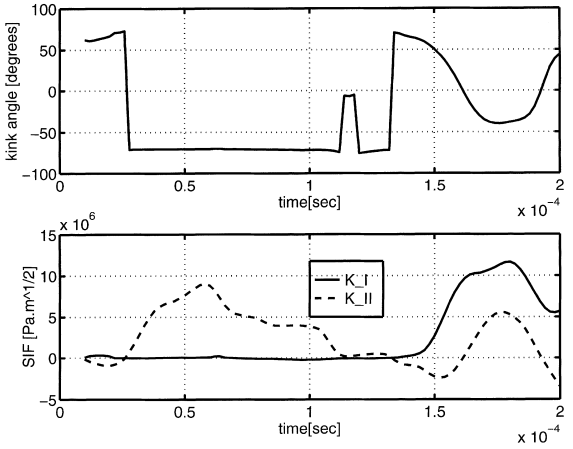

Fig. 9. Prediction of the kink angle based on the maximum hoop stress determined from a typical evolution of the SIF. During the first 130 μs, the kink angle value will be of 70° corresponding to local opening during almost pure mode II loading. Past this time, mixed-mode loading develops and smaller kink angle values are predicted.

shear band may have preceded the opening failure stage. Adiabatic shear banding of course does not obey a normal stress criterion and it was proposed by Rittel and Levin (1998) that a critical value of the mode II SIF triggers its formation (4 MPa $m^{1/2}$).

Our present experiments complement the previous suggestion by requiring that the material be locally heated to a level promoting shear band formation and shear failure. This temperature can be identified as T_g (Tetelman and Mac Evily, 1967), or to the neighboring softening temperature. Consequently, it appears that different failure criteria compete to dictate the response of the same material as evidenced from the different failure mechanisms which operate.

In contrast with polycarbonate, we did not observe such a velocity related transition including shear band formation with polymethylmethacrylate (PMMA) specimens ($T_g = 100°C$) tested at room temperature (Rittel and Maigre, 1996b). Additional preliminary experiments, similar to those reported here, were carried out at approximate equivalent temperatures [in K] of 0.9 T_g and 1.13 T_g. The impact velocity was about 55 m/s. For the specimen heated to 0.9 T_g, fracture occurred at a high kink angle whereas at 1.13 T_g the specimens did not fracture at all, with almost no macroscopic evidence of shear banding. The two polymers are different materials with distinct thermal responses (parallel to Ti6Al4V vs. C300 maraging steel as in Zhou et al., 1996a). Keeping this distinction in mind, the preliminary experiments reinforce the suggestion that local attainment of T_g is nevertheless necessary and sufficient to promote (adiabatic) shear failure in these materials.

The present observations are original in the sense that they clearly show the role and the extent of local crack-tip heating in a material for which there is a well defined notion of thermal transition (T_g). They also illustrate the difficulty in proposing an *isothermal* criterion for dynamic crack initiation in those materials which possess failure mode transitions, in contrast with (brittle) materials for which failure initiates in a direction corresponding to a maximum hoop stress criterion.

Finally, since the transition of failure modes has been originally reported for some metallic alloys, it can be expected that the present methodology should yield useful information about the local temperatures which develop at the crack-tip.

5. Conclusions

Dynamic crack initiation has been investigated in polycarbonate specimens subjected to shear impact loading at various temperatures. All specimens were subjected to almost similar impact velocities of the order of 60 m/s. For this experiment, the loading is initially of pure mode II type (due to contact between the crack faces) followed by mixed-mode loading at later stages (including a positive mode I component).

- The results show that as the baseline temperature is increased from −120°C to −25°C the initial kink angle of 60° decreases to a new value of 40° and less. Specimens tested at room temperature and above do not fail by separation and exhibit significant crack-tip shear banding.
- The transition of failure mode from opening to localized shear is corroborated by scanning electron fractographic analysis showing clearly the presence of a shear band in the specimens frac-

tured at −25°C. The length of the shear band increases from about 200 μm at −25°C to 2–3 mm at +70°C.

- These observations provide a first estimate (lower bound) of local crack-tip elevation of temperature of 175°C by assuming that the crack-tip material has been brought above the glassy temperature of 150°C.
- Significant crack-tip temperature changes put limitations on the usual assumptions of isothermal dynamic crack initiation.

Acknowledgements

This research is supported by the Israel Science Foundation under grant #030-039 and by Technion V.P. Fund for Promotion of Research. Dr. R. Levin's assistance is gratefully acknowledged.

References

ANSYS, 1994. User's Manual, Swanson Analysis Systems Inc.

Barsoum, R.S., 1978. On the use of isoparametric finite elements in linear elastic fracture mechanics. Int. J. Numer. Methods Eng. 10, 25–37.

Bathe, K.J., 1982. Finite Element Procedures in Engineering Analysis. Prentice-Hall, Englewood Cliffs, NJ.

Bui, H.D., Maigre, H., Rittel, D., 1992. A new approach to the experimental determination of the dynamic stress intensity factor. Int. J. Solids and Structures 29 (23), 2881–2895.

Elsevier Materials Selector, 1991. In: Waterman, N., Ashby, M.F. (Eds.), Elsevier, London, p. 1510.

Freund, L.B., 1990. Dynamic Fracture Mechanics. Cambridge University Press, Cambridge.

Kalthoff, J.F., 1988. Shadow optical analysis of dynamic fracture. Optical Engng. 27, 835–840.

Kobayashi, A.S., 1987. Handbook on Experimental Mechanics. Prentice-Hall, Englewood Cliffs, NJ.

Kolsky, H., 1963. Stress Waves in Solids. Dover, New York.

Lawn, B., 1995. Fracture of Brittle Solids, 2nd ed. Cambridge University Press, Cambridge.

Lee, Y.J., Freund, L.B., 1990. Fracture initiation due to asymmetric impact loading of an edge cracked plate. J. Appl. Mech. 57, 104–111.

Lifshitz, J.M., Leber, H., 1994. Data processing in the split Hopkinson pressure bar tests. Int. J. Impact Engng. 15 (6), 723–733.

Mason, J.J., Rosakis, A.J., Ravichandran, G., 1994. Full field measurement of the dynamic deformation field around a growing adiabatic shear band at the tip of a dynamically loaded crack or notch. J. Mech. Phys. Solids 42 (11), 1679–1697.

Nuismer, R.J., 1975. An energy release rate criterion for mixed mode fracture. Int. J. Fracture 11 (2), 245–250.

Ravi-Chandar, K., 1995. On the failure mode transitions in polycarbonate under dynamic mixed mode loading. Int. J. Solids and Structures 32 (6/7), 925–938.

Rittel, D., Maigre, H., 1996a. An investigation of dynamic crack initiation in PMMA. Mechanics of Materials 23, 229–239.

Rittel, D., Maigre, H., 1996b. A study of mixed-mode dynamic crack initiation in PMMA. Mech. Res. Comm. 23 (5), 475–481.

Rittel, D., Levin, R., Maigre, H., 1997. On dynamic crack initiation in polycarbonate under mixed-mode loading. Mech. Res. Comm. 24 (1), 57–64.

Rittel, D., Levin, R., 1998. Mode-mixity and dynamic failure mode transitions in polycarbonate. Mechanics of Materials 30 (3) 197–216.

Tetelman, A.S., McEvily Jr., A.J., 1967. Fracture of Structural Materials. Wiley, New York.

Ward, I.M., Hadley, D.W., 1993. An Introduction to the Mechanical Properties of Solid Polymers. Wiley, Chichester, UK.

Washabaugh, P.D., Knauss, W.G., 1993. Nonsteady periodic behavior in dynamic fracture of PMMA. Int. J. Fracture 59, 187–197.

Zehnder, A.T., Rosakis, A.J., 1991. On the temperature distribution at the vicinity of dynamically propagating cracks in 4340 steel. J. Mech. Phys. Solids, 39 (3), 385–415.

Zhou, M., Rosakis, A.J., Ravichandran, G., 1996a. Dynamically propagating shear bands in impact-loaded prenotched plates. I-Experimental investigations of temperature signatures and propagation speed. J. Mech. Phys. Solids 44 (6), 981–1006.

Zhou, M., Rosakis, A.J., Ravichandran, G., 1996b. Dynamically propagating shear bands in impact-loaded prenotched plates. II-Numerical Simulations. J. Mech. Phys. Solids 44 (6), 1007–1032.